Journal of Science and Technology, Vol. 37, No. 3 (2017), pp32 –45 32

http://dx.doi.org/10.4314/just.v37i3.4

RESEARCH PAPER

MODEL FOR THE PREDICTION AND OPTIMIZATION OF FLAWS AND MATERIAL REMOVAL RATE DURING MACHINING OF SHAFTS IN GHANA

M. K. Boadu[1], **P. Y. Andoh**[2], **A. Agyei-Agyemang**[3] and **P. O. Tawiah**[4]
[2, 3, 4]*Department of Mechanical Engineering, KNUST, Kumasi*
[1]*Department of Mechanical and Industrial Engineering, University for Development Studies, Tamale*

ABSTRACT
The main aim of the study was to develop a prediction model for the flaws and the material removal rate and optimize the cutting conditions during machining using factorial design techniques. A 2^3 experimental design method was used to generate predictive models and plots. The results showed that the feed was the most influencing factor of resistivity (as a measure of intensity and number of flaws) followed by the spindle speed. Depth of cut posed an insignificant influence on resistivity. Similarly, the feed had the highest influence on material removal rate (MRR) followed by depth of cut, and lastly, the spindle speed. The optimal cutting conditions for minimum resistivity was found to be at lower feed (0.2 mm/rev), at higher speed (500 rpm) and at lower depth of cut (1 mm), producing a minimum value of 87.65 μΩ mm resistivity and that of MRR was found to be at lower feed (0.2 mm/rev), higher speed (500rmp) and at higher depth of cut (4 mm) producing a minimum value of 83.25mm^{3}s^{-1} material removal rate. That is the rate of flaw development and/or propagation, and material removal rate during machining of a shaft in Ghanaian manufacturing industries could be modeled and optimized. It can be concluded that there is change in resistivity of materials which can be attributed to increase in the number and intensity of flaws during machining of a shaft and this is influenced by cutting conditions, especially, the feed rate. It is therefore recommended that a feed rate of 0.2mm/rev, a speed of 500 rpm and depth of cut of 1 mm which will give the minimum flaws induced during machining be used.

Keywords: *Machining, turning operation, flaws, material removal rate*

INTRODUCTION

Machining is done by removing unwanted metal parts from a work piece to generate the desired shape. Removal of metal parts is attained by subjecting a specific region of the work piece to fracture (Tapany, 2007). It employs cutting parameters to undergo its operation. Basically there are three cutting parameters, namely: depth of cut, which is distance that the cutting tool penetrates into the work piece;

feed, which involves the transvers movement of the tool relative to the workpiece, and the spindle speed, which is the speed of relative motion between the cutting tool and the work piece in the direction of cutting. Machining uses machine tools such as presses, lathes and power saws. Lathe machines are used to produce cylindrical surfaces through a turning operation. Traditional material removal methods include turning, boring, drilling, reaming, threading, milling, shaping, planning, broaching, and abrasive methods such as grinding, ultrasonic machining, lapping, and honing. Non-traditional methods involve electrical and chemical means of machining, as well as the use of abrasive jets, water jets, laser beams, and electron beams (Kalpakjian, 2006). The shape of the work surfaces is constrained to circular or flat shapes.

Shafts are mostly used to transmit power from one part of a machine to another. The shafts need to be resilient enough to be able to transmit power and torque efficiently and with high reliability in machinery. In the automobile industry, longitudinal shafts play a major role in delivering torque from the engine to other parts of the car. This function cannot be performed by any other machine element except the shaft. Success in the use of shafts in engine construction has increased their demand and, for that matter, the need to investigate the effects that their manufacturing process has on its structural integrity.

The production of machine parts, especially shafts is mainly done by machining. The severity of the machining process could reduce or advance crack growth, according to Benachour *et al*. (2015). It is therefore of extreme importance to know how different cutting parameters affect the introduction and increase in the number of flaws including crack initiation and its growth, in order to optimize them to reduce if not to eliminate their negative influence.

In spite the advances in machining cracks, and for that matter flaws, still pose a significant threat to newly manufactured shafts. As crack growth reaches a maximum level, total failure may occur causing breakdown of machines which could subsequently injure machine operators and even cause death in extreme cases. Moreover, manufacturing firms usually incur huge cost in the production of new shafts when higher number of flaws and crack signatures in their already manufactured shafts are discovered. It is also of no doubt that selection of suitable cutting parameters for machining is a major problem for many machinists. They may not know which cutting conditions to choose and why they are chosen during machining.

Basically, crack growth is defined as an extension in the discontinuities of a material. Crack initiation and growth in rotating machinery is due to the stresses, strains, heat gradients and forces exerted on the member. If a material is under tension, the stresses on the material act in such a way that they pull apart the molecules that make up the material. If the material is under compression, the stresses push the molecules together causing it to be shorter in length as per Nyberg (2007). Cracking of shafts occurs as a result of different factors including high and low cycle fatigue, or stress corrosion.

Silva (2003) studied the flaw generated in two crankshafts of a diesel van which were utilized for 30,000 km and then machined. After the machining process, the two crankshafts lasted only for 1,000 km and failed. As a result of wrong machining process, tiny fatigue cracks formed along the center of the crankshaft causing it to fail. The cracks were sharp and invisible in nature. The investigation was also upheld by determining the other damage modes of crankshaft.

Katsuyama *et al.* (2011) performed surface machining analysis and his results revealed that tensile residual stress resulting from surface machining only occur approximately 0.2 mm from the machined surface, and the surface residual stress advances with spindle speed. The crack growth analysis denoted that the crack depth was influenced by both surface machining and welding. The crack length was found to be highly affected by surface machining than by welding.

Mourad *et al*. (2009) presented an experimental prove of the influence of machining process on stable crack growth behaviour (SCG) of an

AISI 4340 low alloy steel. The load-load displacement (P-ΔLL) curves denote that the "normal" sample showing stable crack growth and the non-linear area, in the anomalous curve of the anomalous sample, is rather restricted.
Shen and Lei (2005) applied a distinct element method (DEM) to simulate the material removal method of laser aided machining of silicon nitride ceramics and showed the generation and extension of surface/sub-surface cracks and damage. It was found that factors such as temperature, rake angle, depth of cut, local damping coefficient and cluster size influence surface/sub-surface cracks.

Benachour *et al*. (2015) presented a paper showing the impact of machining mode of the notch on fatigue crack growth and fractured surfaces. The results denote that the fatigue crack growth is influenced by machining process.

In an investigation of fracture of cementitious composite materials, Veselý *et al*. (2014a) and Konečný *et al.* (2014) established that fracture and flaws generally have influences on the resistivity of materials. This was later confirmed with new results from supplementary tests conducted under different moisture conditions by Veselý *et al*. (2014b). In a study, Bogdanov *et al*., (2000) using an electrical-resistivity method simulated flaws with controlled dielectric inclusions to establish the presence of flaws. Their tests revealed that the apparatus reliably detects flaws that break the surface and subsurface flaws down to a depth of 2.5 mm. Bogdanov *et al*., 2000). The feasibility of electrical-impedance method of flaw detection was also established by Ludwig *et al*., (1998) and Ikeda *et al*., (1991). It is therefore well known that the resistivity of materials gives a measure of the intensity of flaws inherent it.

The method of factorial design gives a way by which one can plan, execute, evaluate and actually substantiate experiments so as to enable real and clear conclusions to be attained correctly and economically. Experimenters through factorial design are able to obtain a larger understanding and authority over the procedure of the experiment. It has seen wide applications in industrial settings since it is able to improve the quality of products and process systems (Anthony and Capon, 1998). Factorial design allows the determination of main and interaction effects of the process variables on dependent parameters, and thus, the importance of the effects are judged. Hence, the objective of this research is to develop a prediction model for the flaws and crack growth and the material removal rate and optimize the cutting conditions during machining using factorial design techniques.

MATERIALS AND METHODS

Work piece material

The work piece material used for present work was cold drawn AISI 1020 mild steel. Table 1 and Table 2 show the chemical composition and mechanical properties, respectfully, of AISI 1020. It was selected for the machining operation because it is referred to by the American Iron and Steel Institute (AISI) as a standard shaft material. It has high machinability, high

Table 1: **Chemical composition of AISI 1020CD**

Element	Content
Carbon, C	0.17 - 0.230 %
Iron, Fe	99.08 - 99.53 %
Manganese, Mn	0.30 - 0.60 %
Phosphorous, P	≤ 0.040 %
Sulfur, S	≤ 0.050 %

Source: AZoM, 2012

Table 2: **Properties of AISI 1020CD**

Physical properties	Metric
Density	7.87 g/cc
Hardness, Brinell	111
Hardness, Knoop (Converted from Brinell hardness)	129
Hardness, Rockwell B (Converted from Brinell hardness)	64
Hardness, Vickers (Converted from Brinell hardness)	115
Tensile Strength, Ultimate	394.72 MPa
Tensile Strength, Yield	294.74 MPa
Elongation at Break (in 50 mm)	36.50%
Reduction of Area	66.00%
Modulus of Elasticity (Typical for steel)	200 GPa
Bulk Modulus (Typical for steel)	140 GPa
Poisson Ratio	0.29

Source: AZoM, 2012

strength, high ductility and good weldability. As a result of its low carbon content, it is resistant to induction hardening or flame hardening. It has extensive applications in industry so as to improve weldability or machinability characteristics. It is utilized in a series of applications because of its cold drawn or turned and polished finish feature (AZoM, 2018).

Selection of control factors

In this study, cutting experiments are planned using statistical two-level full factorial experimental design. Cutting experiments are conducted considering three cutting parameters: Feed rate (mm/rev), cutting Speed (rev/min), depth of cut (mm) and overall 16 experiments were carried out. Table 3 shows the values of various parameters used for experiments:

Experimental method procedure

Turning is a popularly used machining process. The CNC machine plays a major role in modern machining industry to enhance and increase productivity within less time. Fig. 1 shows the CNC machine used for the turning operation.

Each work piece was cut to a size of 43 mm diameter and 400 mm length and the turning operation performed on CNC turning centre. Turning program was prepared and fed to the CNC machine. In this work, the Direct Current Potential Drop (DCPD) method was used to measure the resistance induced before and after each of the turning operation. A weighing machine was used for measuring the initial and final weight of the work piece and the results noted. Machining time was measured using a

Table 3: The Experimental matrix

Variables	Lower Level (-)	Upper Level (+)
Feed Rate, f (mm/rev)	0.20	0.80
Spindle Speed, v (rev/min)	200	500
Depth of Cut, d (mm)	1.00	4.00

Fig. 1: Forceturn 800.50 lathe machine

stopwatch and the results noted. The resistivity is calculated by using the relation $\rho = \frac{\pi R d^2}{4L}$,

where, d is the diameter of the work piece (mm), L is the length of the work piece (mm), R is the resistance measured (μΩ). The change in resistivity is calculated using $\Delta\rho = \rho_f - \rho_i$ where ρ_i is the initial resistivity and ρ_f is the final resistivity. Similarly, the material removal rate is calculated by using the relation

$M = \frac{W_i - W_f}{\rho_d T}$, where, W_i is initial weight of the work piece (g), W_f is final weight of the work piece (g), T is the machining time (sec) and ρ_d is the Density of material (kg/m^3).

At each setting condition, the initial and final resistance, the initial and final weight as well as machining time were recorded. The averages of the two runs were computed for each set of conditions. Table 4 shows the magnitude of the change in resistivity and the material removal rate responses.

The computed averages are used as the responses for each condition in calculating the main effects and the interaction effects for each response. The major goal of these experiments is to determine which of the responses are influenced by the cutting parameters and to generate a model that may be used to predict the resistivity, and for that matter, the intensity and for that matter, the intensity and number of flaws during machining.

ANALYSIS AND DISCUSSION OF RESULTS

Computation of effects and the standard error

The main effect of each of the process variables reflects the changes of the respective responses as the process variables change from a low to a high level. The computed average of the four measures is the main effect of the factor (variable). The formulas used for the computations are as listed in equations 1 through 13.

The main effect of the feed rate is

$$E_f = \frac{1}{4}\{(R_2 + R_4 + R_6 + R_8) - (R_1 + R_3 + R_5 + R_7)\} \quad (1)$$

The main effect of the cutting speed is:

$$E_v = \frac{1}{4}\{(R_3 + R_4 + R_7 + R_8) - (R_1 + R_2 + R_5 + R_6)\} \quad (2)$$

The main effect of the depth of cut is:

$$E_d = \frac{1}{4}\{(R_5 + R_6 + R_7 + R_8) - (R_1 + R_2 + R_3 + R_4)\} \quad (3)$$

Two or more of the variables may jointly influence the responses. These joint influences are referred to as interactions. These interactions are given as follows:

The interaction between the feed rate and the cutting speed is defined as:

$$I_{fv} = \frac{1}{4}\{(R_1 + R_4 + R_5 + R_8) - (R_2 + R_3 + R_6 + R_7)\} \quad (4)$$

The interaction between the feed rate and the depth of cut is defined as:

$$I_{fd} = \frac{1}{4}\{(R_1 + R_3 + R_6 + R_8) - (R_2 + R_4 + R_5 + R_7)\} \quad (5)$$

The interaction between the cutting speed and the depth of cut is defined as:

$$I_{vd} = \frac{1}{4}\{(R_1 + R_2 + R_7 + R_8) - (R_3 + R_4 + R_5 + R_6)\} \quad (6)$$

The three-factor interaction is expressed as

$$I_{fvd} = \frac{1}{4}\{(R_2 + R_3 + R_5 + R_8) - (R_1 + R_4 + R_6 + R_7)\} \quad (7)$$

The mean of the runs is defined as

$$E_M = \left[\sum_{1}^{8} R_i \Big/ 8\right] \quad (8)$$

where R_i are the responses (resistivity and material removal rate). The estimates for the two responses are shown in Table 5.

When genuine run replicates are created under a given set of experimental conditions, the variation among their associated observations are used to estimate the standard deviation of a single observation and, hence, the standard deviation of the results. In general, if g sets of experimental conditions are genuinely replicated and the n_i replicate runs made at the i^{th} set yield an estimate s_i^2 having $v_i = n_i - 1$ degree (s) of freedom (Hunter, 1978), the estimate of

Table 4: Values for the change in Resistivity (Δρ) and Material Removal Rate (M) Responses

Points	Code			Resistivity (μΩm)			Material Removal Rate (mm^3/s)		
	f	v	d	Run 1	Run 2	Mean	Run 1	Run 2	Mean
1	-	-	-	102.86	106.96	Δρ=104.91	88.5	87.9	M= 88.20
2	+	-	-	181.23	171.86	Δρ=176.54	352.4	353.7	M= 353.05
3	-	+	-	86.69	88.60	Δρ=87.65	219.7	223.4	M=221.55
4	+	+	-	132.97	129.47	Δρ=131.22	86.5	87.4	M=86.95
5	-	-	+	158.68	159.63	Δρ=159.16	323.5	326.7	M= 325.1
6	+	-	+	202.47	171.01	Δρ=186.74	130.7	135.3	M= 133.00
7	-	+	+	158.02	163.03	Δρ=160.52	81.6	84.9	M=83.25
8	+	+	+	177.00	175.03	Δρ=176.01	330.2	328.5	M=329.35

Note: (-) represents the lower level of the variables, (+) represents the upper level of the variables

run variance is

$$s^2 = \frac{v_1 s_1^2 + v_2 s_2^2 + v_3 s_3^2 + \ldots + v_g s_g^2}{v_1 + v_2 + v_3 + \ldots + v_g} \quad (9)$$

With only $n_i = 2$ replicates at each of the g sets of conditions, the formula for the i^{th} variance reduces to

$$s_i^2 = d_i^2 / 2 \quad (10)$$

with $v_i = 1$, where d_i is the difference between the duplicate observations for the ith set of conditions. Thus, equation 9 will yield

$$s^2 = \sum \left(d_i^2 / 2 \right) / g \quad (11)$$

In general, if a total of N runs is made conducting a replicated factorial design, then the variance of an effect is given as

$$V(effect) = \frac{4}{N} s^2 \quad (12)$$

and the standard error of the effect is given as

$$s_e = \sqrt{V(effect)} \quad (13)$$

DISCUSSION OF RESULTS

The major and most important part of the results in the study are the effects. The three main effects (feed rate, f, spindle speed, v and depth of cut, d), the two-factor effect being a measure of the interactions of any two variables and the three-factor interaction effect, feed rate, spindle speed and depth of cut were estimated using the mean of the runs. Table 5 summarizes the findings.

Identification of important effects

The objective is to select factors that have large effects on the responses by creating a factorial design and collecting the response data to fit a model. The response data collected is used to generate graphs to evaluate the effects. The use of the output from fitting a mathematical model, and also the use of the two graphical methods to help see which factors are important for optimizing the resistivity and the material removal rate during machining process. The main effects (feed, speed and depth of cut) and the interaction plots were generated for both the resistivity and the material removal rate and are presented in Figs. 2 and 3 respectively.

Table 5: Coefficient of analysis for the two responses

Term	Resistivity				Material Removal Rate			
	Effect	Coef	SE Coef	Status	Effect	Coef	SE Coef	Status
Constant		6.66	0.08	Real		202.56	0.49	Real
f	3.8	1.9	0.08	Real	46.06	23.03	0.49	Real
v	-1.96	-0.98	0.08	Real	-44.56	-22.28	0.49	Real
d	0.22	0.11	0.08	Chance	30.24	15.12	0.49	Real
fv	-1.24	-0.62	0.08	Real	9.69	4.84	0.49	Real
fd	-0.64	-0.32	0.08	Real	-19.06	-9.53	0.49	Real
vd	0.44	0.22	0.08	Real	21.81	10.91	0.49	Real
fvd	-0.18	-0.09	0.08	Chance	209.41	104.71	0.49	Real

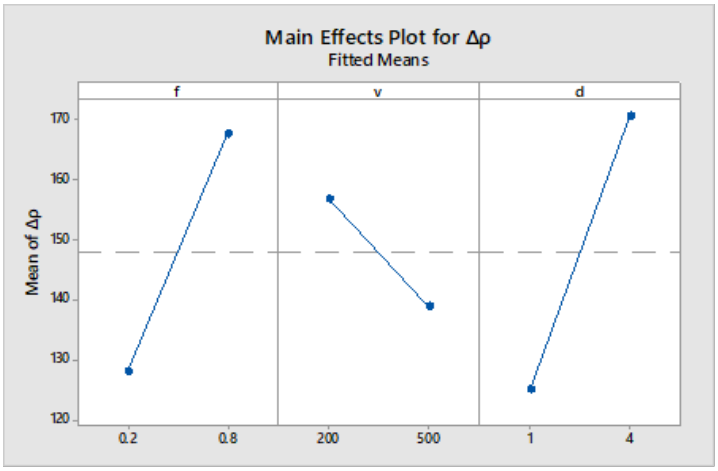

Fig. 2: Main effects plot for change in resistivity (Δρ)

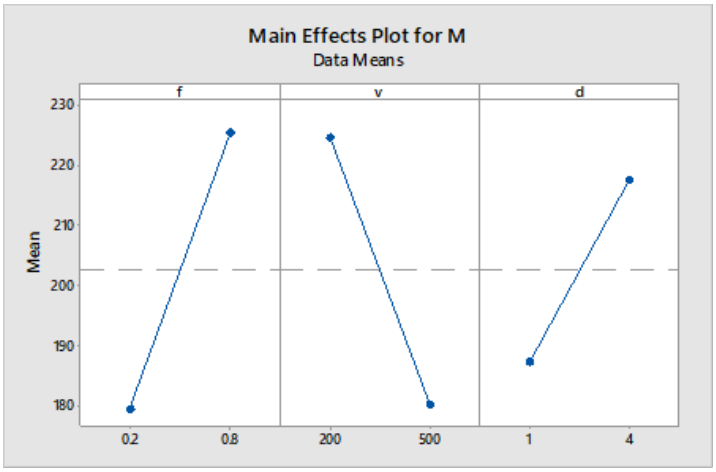

Fig. 3: Main effects plot for material removal rate (M)

The main effect plot shows the degree of an effect at low and high levels. The resistivity is low (128.06 μΩmm) when the feed rate is 0.2 mm/rev, and high (167.63 μΩmm) when the feed rate is 0.8 mm/rev. This implies that the resistivity increases with increasing feed. The resistivity is also low (138.85 μΩmm) when the speed is 500 rpm, but high (156.84 μΩmm) when the speed is 200 rpm. This denotes that the resistivity increases by reducing the speed. The resistivity is low (125.08 μΩmm) when the depth of cut is 1 mm and quiet high (170.61 μΩmm) when the depth of cut is 4 mm. Similarly, the material removal rate (MRR) is low

(179 mm^3/min) when the feed rate is 0.2 mm/rev and high (226 mm^3/min) when the feed rate is 0.8 mm/rev. This implies that the MRR increases with increasing the feed. The MRR is also low (180 mm^3/min) when the speed is 500 rpm and high (225 mm^3/min) when the speed is 200 rpm. This denotes that the MRR increases by decreasing the speed. The MRR is low (187 mm^3/min) when the depth of cut is 1 mm and high (218mm^3/min) when the depth of cut is 4 mm. This also denotes that the MRR increases as the depth of cut increases.

Fig. 4 shows the graphical illustration of interaction effects of the cutting parameters on resistivity and the material removal rate. The plot examines two-way interactions. The plot also assesses the lines to comprehend how interactions influence the response. The dotted lines represent low levels and the straight lines represent high levels of the independent variables.

The feed-speed interaction is significant and has the strongest strength of interaction since the lines greatly depart from being parallel. The feed-depth of cut interaction is also significant and has a stronger strength of interaction. The speed-depth of cut interaction is statistically significant since its lines are not parallel and thus, has the least strength of interaction.

Fig. 5 shows a Pareto chart of the standardized effects of feed, speed and depth of cut at 95% confidence level α is taken to be 0.05. The Pareto chart is another helpful tool to ascertain the significance of the effects. It uses the phenomenon of the normal plot of standardized effects. The effect or factor becomes significant if it crosses the reference line. The effect becomes insignificant if it does not cross the reference line. For the resistivity, the depth of cut is significant with the highest absolute standardized effect of 10.8, and feed-speed interaction is significant with the lowest absolute standardized effect of 2.38, since both crosses the reference line of 2.31.

The three factor interaction (feed-speed-depth of cut) is insignificant with an absolute standardized effect of 0.95, and that showed the least influence on resistivity. However, for the material removal rate both the main effects and the interactions are having significant effects; the feed-speed-depth is significant with the highest absolute standardized effect of 220, and speed-depth of cut interaction is significant with the

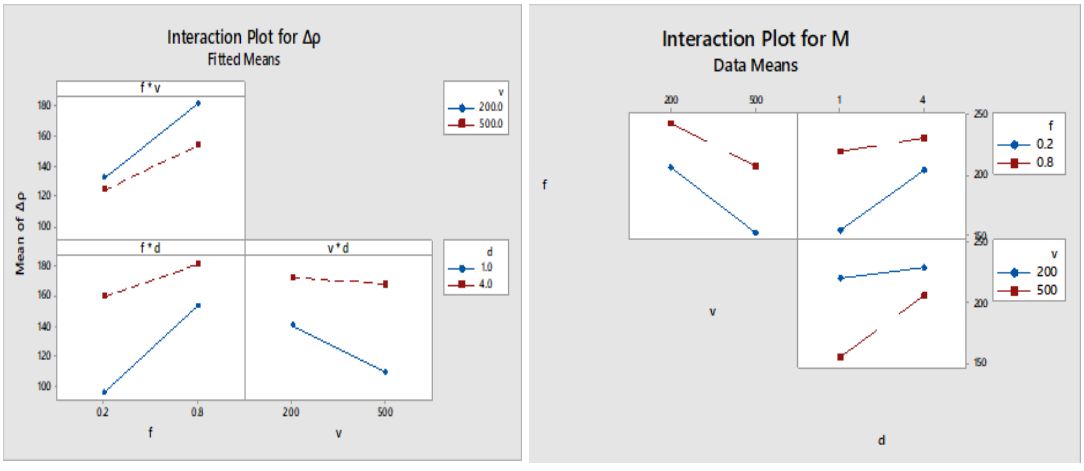

Fig. 4: Interaction plot for change in resistivity (Δρ) and material removal rate (M)

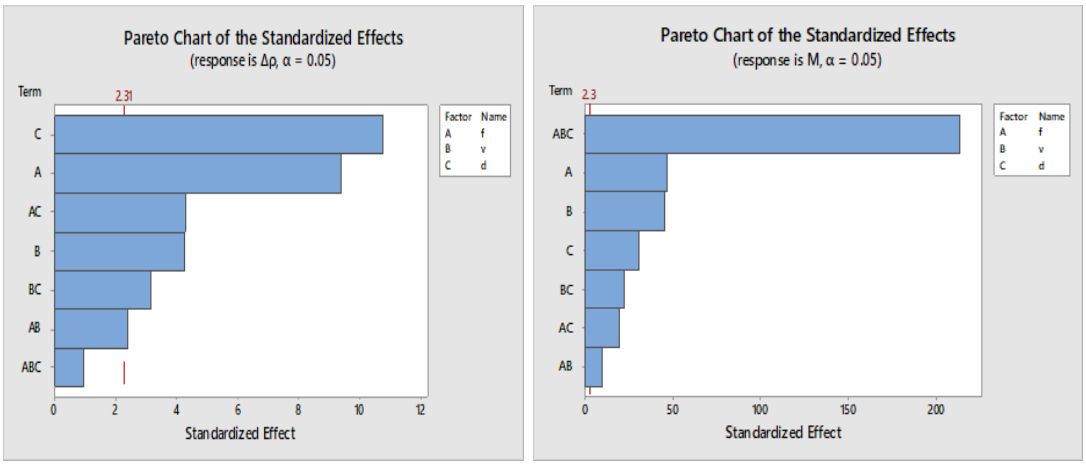

Fig. 5: Pareto chart of standardized effects

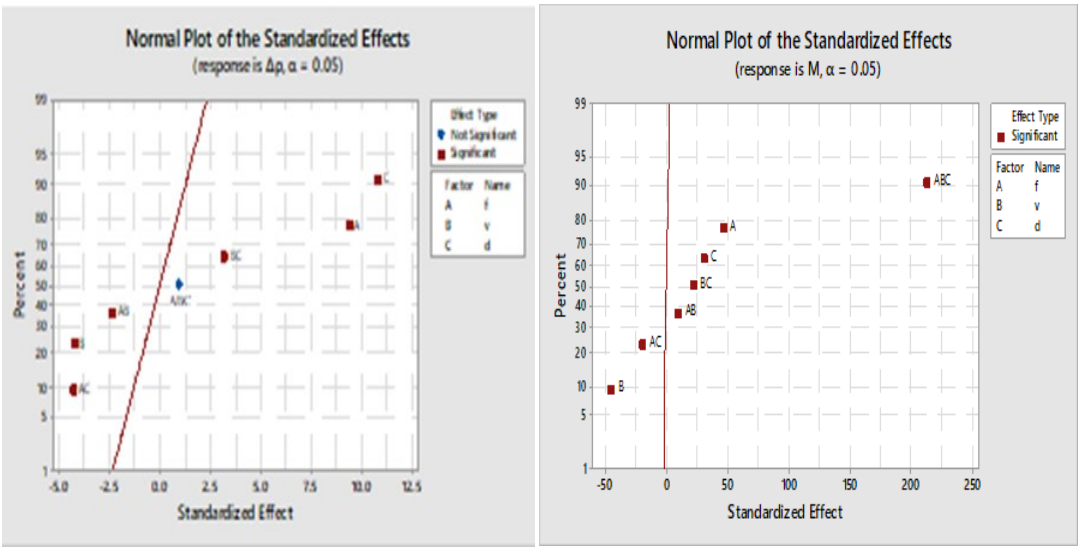

Fig. 6: Norm plot of standardized effects

lowest absolute standardized effect of 15, since both crosses the reference line of 2.31.

Fig. 6 shows the normal plot of the standardized effects on resistivity. The normal plot shows the statistical significance and direction of the main and interaction effects as well as their percentage on the response variable at 95% confidence level and at $\alpha = 0.05$. The closer the factor is to the reference line, the less significant its effect becomes and the farther the factor is from the line the more significant

its effect becomes. Any factor which lies on the reference line has a completely insignificant effect.

For the resistivity, the effect of feed, depth of cut and the speed-depth interactions are significant in the positive direction which means that the three effects increase with increasing resistivity. The effect of speed, feed-speed interaction and feed-depth of cut interaction are statistically significant in the negative direction and this shows that as these effects increase, resistivity decreases. However, the three factor interaction are statistically insignificant since is close to the reference line.

Similarly, for the material removal rate, the effect of speed, and feed-depth of cut interaction are statistically significant in the negative direction and this shows that as these effects increase, the material removal rate decreases. The remaining five effects are significant in the positive direction which means that these effects increase with increasing material removal rate.

Generation and evaluation of prediction model

A full 2^3 model consist of three main effects, three two factor interactions and one three-factor interaction. It is easier to obtain residuals from a 2^3 design by fitting a regression model to the data. For this experiment, the model is defined as:

$$R = \beta_0 + \beta_1 f + \beta_2 v + \beta_3 d + \beta_4 fv + \beta_5 fd + \beta_6 vd + \beta_7 fvd \quad (14)$$

where

$$\beta_0 = mean; \quad \beta_1 = \frac{E_f}{2}; \quad \beta_2 = \frac{E_v}{2}; \quad \beta_3 = \frac{E_d}{2};$$
$$\beta_4 = \frac{I_{fv}}{2}; \quad \beta_5 = \frac{I_{fd}}{2}; \quad \beta_6 = \frac{I_{vd}}{2}; \quad \beta_7 = \frac{I_{fvd}}{2} \quad (15)$$

The significant effects and interactions were used to develop the empirical model for the responses with the use of Equations 13 and 14 and Table 5. Thus, the models for the two responses are

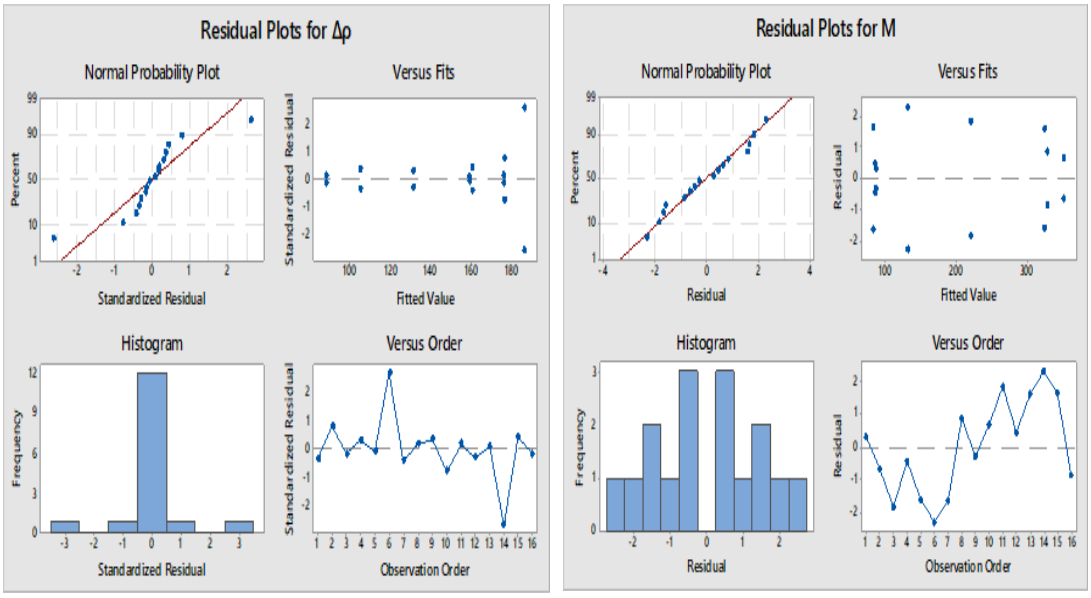

Fig. 7: Residual plots for change in resistivity (Δρ) and material removal rate (M)

$$\Delta\rho = 66.3 + 181f - 0.412v + 20.02d - 0.1855fv - 30.4\,fd + 0.0148vd + 0.0296\,fvd \quad (16)$$

$$M = -452.91 + 1449.35\,f + 1.62v + 275.16d - 3.77\,fv - 564.10\,fd - 0.73\,vd + 1.55\,fvd \quad (17)$$

The models were evaluated by generating plots to visualize the effects, evaluate the fit of the reduced model, and also do a residual analysis. A good standard by which to evaluate the model is to look at p-values. The fitted values are the results predicted by the model and the residuals are the actual values minus the predicted values. The results obtained are presented in Fig. 7.

As illustrated in Fig .7, the residual error only increased by a small amount and also, the p-value for each term in the model is less than 0.05, indicating that the two models are good candidates for further exploration and validation. Also, the residuals plots were satisfactory, and showed no cause for concern. Therefore, the models developed are considerably simpler and fit the data almost as well as the models with all terms.

Optimization of the Model

The optimization plots were generated and the results are illustrated in Fig. 8.

From the plot, it can be seen that the optimal

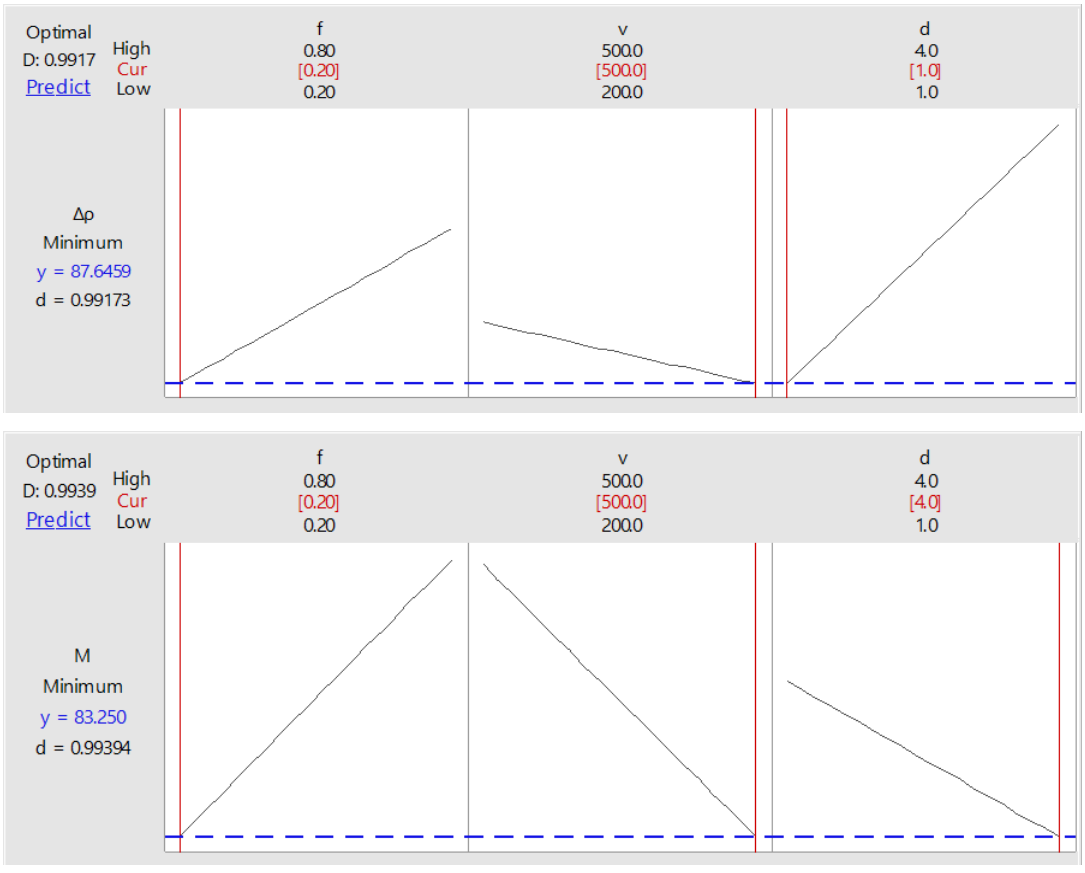

Fig. 8: Optimization plots of change in Resistivity (Δρ) and Material removal rate

cutting conditions for resistivity are indicated in bracket with the values of 0.2 mm/rev for the feed rate, 500 rpm for the speed and 1 mm for depth of cut producing a minimum value of 87.65 μΩmm resistivity. Similarly, for the material removal rate, the optimal cutting conditions are 0.2 mm/rev for the feed rate, 500 rpm for the speed and 4 mm for depth of cut producing a minimum value of 83.25 mm^3s^{-1} material removal rate.

CONCLUSIONS

The study is to investigate the amount of flaws induced and/or propagated, the material removal rate and the effects of cutting parameters on these responses during machining of shaft. During the experiments $\Delta\rho$ was positive, therefore the flaw intensity increased as a result of machining. It is concluded that, flaw development and/or propagation, and material removal rate during machining of a shaft in Ghana Manufacturing industries can be modeled and optimized. The predicted model obtained for the resistivity and the material removal rate are

$\Delta\rho = 66.3 + 181f - 0.412v + 20.02d - 0.1855fv - 30.4\ fd + 0.0148vd + 0.0296\ fvd$ and $M = -452.91 + 1449.35\ f + 1.62v + 275.16d - 3.77\ fv - 564.10\ fd - 0.73\ vd + 1.55\ fvd$ respectively. Finally, the optimal cutting conditions for resistivity are at lower feed (0.2 mm/rev), at higher speed (500 rpm) and at lower depth of cut (1 mm) producing a minimum value of 87.65 μΩ mm resistivity and material removal rate, are at lower feed rate (0.2 mm/rev), at higher speed (500 rpm) and higher depth of cut (4 mm) producing a minimum value of 83.25 mm^3s^{-1} material removal rate. It can therefore be recommended that a federate of 0.2 mm/rev, at a speed of 500 rmp and a depth of cut of 1 mm, which will give the minimum flaws induced during machining, be used.

REFERENCES

Antony, J. and Capon, N.(1998). Teaching Experimental Design Techniques to Industrial Engineers. *International Journal of Engineering Education, Tempus Publications, 14 (5): 335-343*

Azom, ? (2012), AISI 1020 Low Carbon/Low Tensile Steel. Source: URL: https://www.azom.com/article.aspx?ArticleID=6114

Benachour, M., Benachour, N. and Benguediab, M. (2015). "Effect of Machining Mode of Notch on Fatigue Crack Growth and Fractured Surfaces". *International Journal of Materials Chemistry and Physics, 1 (2): 198-201*

Bogdanov, G., Ludwig, R. and Michalson, R. W. (2000). A new apparatus for non-destructive evaluation of green-state powder metal compacts using the electrical-resistivity method. Measurement Science and Technology, 11: 157–166

eFunda (2017). www.efunda.com/materials/alloys/carbon_steels/show_carbon.cfm?id=aisi_1020&prop=all&page_title=aisi%201020 (accessed: May 10, 2017)

Ikeda, K., Yoshimi, M. and Miki, C. (1991). Electric potential drop method for evaluating crack depth. *International Journal of Fracture, 47: 25–38*

Kalpakjian, S. (2006). Manufacturing Engineering and Technology, Fifth Edition, Prentice Hall Publishing Co.

Konečný, P., Veselý, V., Lehner, P., Pieszka, D. and Žídek, L. (2014). Investigation of selected physical parameters of cementitious composite during sequential fracture test. Advanced Materials Research, 969: 228–233 doi:10.4028/www.scientific.net/AMR.969.228.

Ludwig, R., Makarov, S and Apelian, D. (1998). Theoretical and practical investigations of electric resistivity testing of green-state P/M compacts. *Journal of Nondestructive Evaluation,17: 153–66*

Mourad, A. I. and Aladdin, A. (2009). "Effect of Machining Process on Stable Crack Growth", ASME Pressure Vessels and Piping Conference, Vol 6, Paper No. PVP2009-78085, pp. 197-202

Nyberg, C. (2007). "Understanding factors that cause shaft failures". Pumps and Systems,

published by the Cahaba Media Group, Birmingham, UK

Ihara,R.,Katsuyama, J., Onizawa, K.,Hasimoto, T., Mikami, Y. and Mochizuki, M. (2011). "Prediction of residual stress distributions due to surface machining and welding and crack growth simulation under residual stress distribution". Nuclear Engineering and Design, 241 (5): 1335–1344.

Shen, X and Lei, S. (2005). "Distinct Element Simulation of Laser Assisted Machining of Silicon Nitride Ceramics: Surface/Subsurface Cracks and Damage", ASME International Mechanical Engineering Congress and Exposition, Paper No. IMECE2005-80545, pp.1267-1274

Silva, F.S. (2003). "Analysis of Vehicle Crankshaft Failure". Engineering Failure Analysis, 10: 605-616.

Tapany, U. (2007). "Machining of Metals Subjects of Interest pps.", Lecture at Suranaree University of Technology, pp. 2- 4

Veselý, V., Konečný, P., Lehner, P., Pařenica, P., Hurta, J. and Žídek, L. (2014a). Investigation of fracture and electrical resistivity parameters of cementitious composite for their utilization in deterioration models. Key Engineering Materials, 577–578: 265–268. doi:10.4028/www.scientific.net/KEM.577-578.265.

Veselý ,V., Konečný, P., Lehner, P., Pieszka, D. and Žídek, L. (2014b). Electrical resistivity and ultrasonic measurements during sequential fracture test of cementitious composite. Frattura ed Integrità Strutturale, 30: 263-272